THE JOURNAL OF BIOLOGICAL CHEMISTRY VOL. 285, NO. 34, pp. 26369–26376, August 20, 2010

Regulation of AMPA Receptor Trafficking and Function by Glycogen Synthase Kinase 3*[S]

Received for publication, March 8, 2010, and in revised form, June 17, 2010 Published, JBC Papers in Press, June 28, 2010, DOI 10.1074/jbc.M110.121376

Jing Wei[‡§1], **Wenhua Liu**[§], **and Zhen Yan**[§2]

From the [‡]*Key Laboratory of Developmental Genes and Human Disease, Ministry of Education, Institute of Life Science, Southeast University, Nanjing 210009, Jiangsu Province, China and the* [§]*Department of Physiology and Biophysics, School of Medicine and Biomedical Sciences, State University of New York at Buffalo, Buffalo, New York 14214*

Accumulating evidence suggests that glycogen synthase kinase 3 (GSK-3) is a multifunctional kinase implicated in neuronal development, mood stabilization, and neurodegeneration. However, the synaptic actions of GSK-3 are largely unknown. In this study, we examined the impact of GSK-3 on AMPA receptor (AMPAR) channels, the major mediator of excitatory transmission, in cortical neurons. Application of GSK-3 inhibitors or knockdown of GSK-3 caused a significant reduction of the amplitude of miniature excitatory postsynaptic current (mEPSC), a readout of the unitary strength of synaptic AMPARs. Treatment with GSK-3 inhibitors also decreased surface and synaptic GluR1 clusters on dendrites and increased internalized GluR1 in cortical cultures. Rab5, the small GTPase controlling the transport from plasma membrane to early endosomes, was activated by GSK-3 inhibitors. Knockdown of Rab5 prevented GSK-3 inhibitors from regulating mEPSC amplitude. Guanyl nucleotide dissociation inhibitor (GDI), which regulates the cycle of Rab5 between membrane and cytosol, formed an increased complex with Rab5 after treatment with GSK-3 inhibitors. Blocking the function of GDI occluded the effect of GSK-3 inhibitors on mEPSC amplitude. In cells transfected with the non-phosphorylatable GDI mutant, GDI(S45A), GSK-3 inhibitors lost the capability to regulate GDI-Rab5 complex, mEPSC amplitude, and AMPAR surface expression. These results suggest that GSK-3, via altering the GDI-Rab5 complex, regulates Rab5-mediated endocytosis of AMPARs. It provides a potential mechanism underlying the role of GSK-3 in synaptic transmission and plasticity.

Glycogen synthase kinase 3 (GSK-3),[3] which was initially identified as an enzyme that regulates glycogen synthesis in response to insulin (1), has emerged as a multifunctional serine/threonine kinase involved in many cellular processes, including the proliferation, differentiation, cell adhesion, cell survival and apoptotic signaling, axon growth, neuronal polarity, and neural progenitor homeostasis during development (2–6). There are two closely related GSK-3 isoforms, GSK-3α and GSK-3β, and they are highly enriched in the brain (7). GSK-3 is usually active in resting cells, and its activity can be inhibited by Akt-mediated phosphorylation at N-terminal serine residues (8).

GSK-3 has been implicated in mood disorders (9) because it is the main target of lithium (10), the most effective treatment for manic-depressive illness. Convergent evidence also suggests that impaired Akt-GSK-3β signaling contributes to schizophrenia pathogenesis (11). Moreover, inhibition of GSK-3 has been found to reduce the production of β-amyloid peptides (12) and the hyperphosphorylation of Tau protein (13), two key events in the etiology of Alzheimer disease. Although pharmacological inhibitors of GSK-3 offer great potential for the treatment of a variety of neurological disorders (14), it is important to know the molecular targets and physiological function of GSK-3 in central neurons.

Our previous study has found that the NMDA receptor is one target of GSK-3 (15). Inhibiting GSK-3 activity suppresses NMDA receptor current through a mechanism involving the NMDA receptor internalization (15). GSK-3β has also been found to mediate an interaction between NMDA receptor-dependent long term potentiation and long term depression (16). Because AMPA receptor trafficking is critically involved in the expression of these two forms of synaptic plasticity (17, 18), we sought to determine whether GSK-3 is capable of regulating AMPA receptors, and if so, how this regulation is achieved.

MATERIALS AND METHODS

Primary Neuronal Culture—Rat cortical cultures were prepared as described previously (19, 20). In brief, frontal cortex was dissected from embryonic day 18 rat embryos, and cells were dissociated using trypsin and trituration through a Pasteur pipette. Neurons were plated on coverslips coated with poly-L-lysine in Dulbecco's modified Eagle's medium with 10% fetal calf serum at a density of 1×10^5 cells/cm^2. When neurons attached to the coverslips within 24 h, the medium was changed to Neurobasal medium with vitamin B_{27} supplement (Invitrogen). Cytosine arabinoside (Arac, 5 μM) was added at DIV 3 to stop glial proliferation. Culture neurons (DIV 14–16) were transfected with various plasmids using Lipofectamine 2000 (Invitrogen) method.

Synaptic Current Recording in Neuronal Cultures—Cultured cortical neurons (DIV 16–20) were used for recording AMPAR-mediated miniature excitatory postsynaptic currents (mEPSC) as described previously (20). The external solution

* This work was supported, in whole or in part, by National Institutes of Health Grants NS69929 and MH84233 (to Z. Y.).
[S] The on-line version of this article (available at http://www.jbc.org) contains supplemental Fig. 1X.
[1] To whom correspondence may be addressed. E-mail: jwei83@yahoo.com.cn.
[2] To whom correspondence may be addressed. E-mail: zhenyan@buffalo.edu.
[3] The abbreviations used are: GSK-3, glycogen synthase kinase 3; AMPAR, AMPA receptor; mEPSC, miniature excitatory postsynaptic current; GDI, guanyl nucleotide dissociation inhibitor; DIV, days *in vitro*; DMSO, dimethyl sulfoxide; ANOVA, analysis of variance.

contained (in mM): 127 NaCl, 5 KCl, 2 $MgCl_2$, 2 $CaCl_2$, 12 glucose, 10 HEPES, 0.001 tetrodotoxin, pH 7.3–7.4, 300–305 mosM. The NMDA receptor antagonist D-aminophosphonovalerate (20 μM) and $GABA_A$ receptor antagonist bicuculline (10 μM) were added to the external solution. The internal solution consisted of (in mM): 130 cesium methanesulfonate, 10 CsCl, 4 NaCl, 10 HEPES, 1 $MgCl_2$, 5 EGTA, 2.2 Lidocaine *N*-ethylbromide, 12 phosphocreatine, 5 MgATP, 0.5 Na_2GTP, 0.1 leupeptin, pH 7.2–7.3, 265–270 mosM. The membrane potential was held at −70 mV during recording. Each neuron was recorded continuously for 20–30 min.

Synaptic currents were analyzed with the Mini Analysis program (Synaptosoft, Leonia, NJ). The noise level is below 5 pA, and we usually used 10 pA as the threshold for mEPSC events. Two minutes of representative mEPSC recordings (300–400 events) were used to generate the cumulative distribution plot. Statistical comparisons of synaptic currents were made using the Kolmogorov-Smirnov test. Summary data were presented as mean ± S.E. ANOVA or Student's *t* tests were performed to compare groups subjected to different treatments.

Immunostaining in Neuronal Cultures—Surface AMPA receptors were measured as described previously (20, 21). In brief, cortical cultures were fixed in 4% paraformaldehyde (20 min, room temperature) but not permeabilized. Following the incubation with 5% bovine serum albumin (BSA, 1 h) to block nonspecific staining, neurons were incubated with a polyclonal anti-NT-GluR1 antibody (1:500, Millipore, 07-660) overnight at 4 °C. After washing, neurons were permeabilized and incubated with a monoclonal anti-MAP2 antibody (1:250; Santa Cruz Biotechnology, sc-80013) for 2 h at room temperature. Surface GluR1 was detected with the Alexa Fluor 594 (red)-conjugated anti-rabbit secondary antibody, whereas MAP2 was detected with the Alexa Fluor 488 (green)-conjugated anti-mouse secondary antibody. After washing in PBS three times, coverslips were mounted on slides with VECTASHIELD mounting medium. For the detection of AMPA receptors at synapses, neurons were fixed, permeabilized, and stained with a polyclonal anti-GluR1 antibody (1:500, Millipore, 07-660) and a monoclonal anti-PSD95 antibody (1:500, Abcam, ab-2723) or a polyclonal anti-GluR2/3 antibody (1:500, Millipore, AB1506) and a monoclonal anti-synaptophysin antibody (1:1000, Sigma, S5768) overnight at 4 °C.

The internalized AMPA receptors were detected as described previously (21). Briefly, surface GluR1 was labeled with a polyclonal anti-GluR1 antibody (1:100; Millipore, 07-660) in living cells for 20 min at 37 °C in the culture medium. After washing, neurons were treated with SB216763 (10 μM) or DMSO for 10 min at 37 °C. Following the treatment, the antibody that binds to the remaining surface GluR1 was stripped off with an acid solution (0.5 M NaCl, 0.2 N acetic acid) at 4 °C for 4 min. Cells were then washed, fixed, permeabilized, and incubated with a monoclonal anti-GluR1 antibody (1:200; Santa Cruz Biotechnology, sc-13152) for 2 h at room temperature. The internalized GluR1 (labeled with a polyclonal GluR1 antibody) was detected with the Alexa Fluor 594 (red)-conjugated anti-rabbit secondary antibody, whereas the total GluR1 (labeled with a monoclonal GluR1 antibody) was detected with the Alexa Fluor 488 (green)-conjugated anti-mouse secondary antibody.

Labeled cells were imaged using a 100× objective with a cooled CCD camera mounted on a Nikon microscope. All specimens were imaged under identical conditions and analyzed using identical parameters. The surface GluR1 clusters and internalized GluR1 were measured using the ImageJ software according to our previously described procedures (19–21). To define dendritic clusters, a single threshold was chosen manually so that clusters corresponded to puncta of at least 2-fold greater intensity than the diffuse fluorescence on the dendritic shaft. Three to four independent experiments for each of the treatments were performed. On each coverslip, the cluster density, size, and fluorescence intensity of 4–6 neurons (2–3 dendritic segments of at least 50 μm in length per neuron) were measured. Quantitative analyses were conducted blindly (without knowledge of experimental treatment).

DNA Constructs—Rat GDI-1 open reading frame was cloned from rat brain cDNA by PCR, and a FLAG tag was added in the N terminus of GDI in-frame. Generation of GDI mutants (WT, S45A, S121A, S213A) was carried out with the QuikChange site-directed mutagenesis kit (Stratagene). All constructs were verified by DNA sequencing. GDI constructs (WT, S45A) were co-transfected with enhanced GFP into cortical cultures (DIV 14–16) using the Lipofectamine 2000 method. Two days after transfection, immunostaining or recordings were performed.

Small Interfering RNA—The small interfering RNA (siRNA) for silencing GSK-3α/β (15) or Rab5 (Santa Cruz Biotechnology) was co-transfected with enhanced GFP into cortical cultures (DIV 14–16) using the Lipofectamine 2000 method. Two days after transfection, electrophysiological recordings were performed.

Biochemical Measurement of Surface-expressed Receptors—The surface AMPA receptors were detected as described previously (20). In brief, after treatment, cortical slices were incubated with artificial cerebrospinal fluid containing 1 mg/ml sulfo-*N*-hydroxysuccinimide-LC-Biotin (Pierce) for 20 min on ice. The slices were then rinsed three times in Tris-buffered saline to quench the biotin reaction followed by homogenization in 300 μl of modified radioimmunoprecipitation assay buffer (1% Triton X-100, 0.1% SDS, 0.5% deoxycholic acid, 50 mM $NaPO_4$, 150 mM NaCl, 2 mM EDTA, 50 mM NaF, 10 mM sodium pyrophosphate, 1 mM sodium orthovanadate, 1 mM phenylmethylsulfonyl fluoride, and 1 mg/ml leupeptin). The homogenates were centrifuged at 14,000 × *g* for 15 min at 4 °C. Protein (15 μg) was removed to measure total GluR1. For surface protein, 150 μg of protein was incubated with 100 μl of 50% NeutrAvidin-agarose (Pierce) for 2 h at 4 °C, and bound proteins were resuspended in 25 μl of SDS sample buffer and boiled. Quantitative Western blots were performed on both total and biotinylated (surface) proteins using anti-GluR1 antibody (1:500; Millipore, 07-660), anti-GluR2 antibody (1:500, Millipore, MAB397), or anti-$GABA_A$ receptor antibody (1:500, Millipore, MAB341).

Co-immunoprecipitation—Slices or transfected HEK293T cells were collected and homogenized in Nonidet P-40 lysis buffer. Lysates were ultracentrifuged (200,000 × *g*) at 4 °C for 1 h. Supernatant fractions were incubated with anti-Rabaptin-5

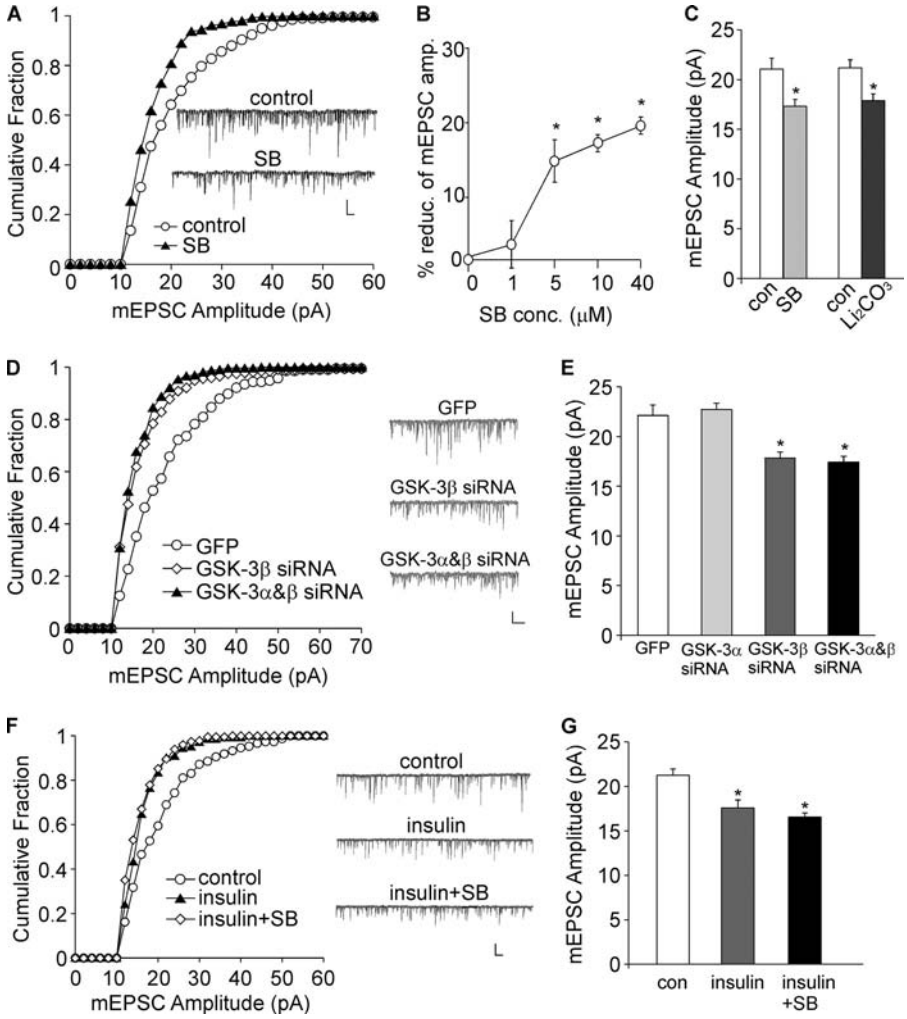

FIGURE 1. **Inhibiting GSK-3 reduces synaptic AMPAR responses.** *A*, cumulative plots of mEPSC amplitude distribution before (*control*) and after SB216763 (*SB*, a GSK-3 inhibitor, 10 μM) treatment in a cultured cortical neuron. *Inset*, representative mEPSC traces. *Scale bar*, 20 pA, 1 s. *B*, dose-response data showing the percentage reduction of mEPSC amplitude by different concentrations of SB216763 (*SB conc.*). *C*, bar graphs showing the mEPSC amplitude in neuronal cultures treated with or without GSK-3 inhibitors (SB216763, 10 μM; Li_2CO_3, 1 mM). *con*, control. *, $p < 0.01$, ANOVA. *D*, cumulative plots of mEPSC amplitude distribution in cultured cortical neurons transfected with GFP, GSK-3β siRNA, or GSK-3α and GSK-3β siRNAs. *Inset*, representative mEPSC traces. *Scale bar*, 20 pA, 1 s. *E*, bar graph showing the mEPSC amplitude in neurons transfected with different siRNAs. *, $p < 0.01$, ANOVA. *F*, cumulative plots of mEPSC amplitude distribution in cultured cortical neurons treated with insulin (0.5 μM) or insulin plus SB216763. *Inset*, representative mEPSC traces. *Scale bar*, 20 pA, 1 s. *G*, bar graphs showing the mEPSC amplitude in neurons treated with different agents.

antibody (5 μg; Santa Cruz Biotechnology, sc-15351), anti-GDI antibody (5 μg; Synaptic Systems, 130011), or anti-FLAG antibody (1:100, Sigma, F3165) overnight at 4 °C followed by incubation with 50 μl of protein A/G plus agarose (Santa Cruz Biotechnology) for 1 h at 4 °C. Immunoprecipitates were washed three times with lysis buffer containing 0.2 M NaCl and then boiled in 2× SDS loading buffer for 5 min and separated on 10% SDS-polyacrylamide gels. Western blotting experiments were performed with anti-Rab5 antibody (1:500; Santa Cruz Biotechnology, sc-28570) or anti-Rab4 antibody (1:1000, BD Biosciences, 610888).

RESULTS

GSK-3 Regulates Synaptic AMPAR Currents in Cultured Cortical Neurons—To examine the role of GSK-3 in AMPAR-mediated synaptic responses, we treated cortical cultures with GSK-3 inhibitors and measured mEPSC, a response from quantal release of single glutamate vesicles. A significant change in mEPSC amplitude often suggests a modification of postsynaptic AMPA receptors. As shown in Fig. 1*A*, application of SB216763 (10 μM, 10 min), a potent and selective GSK-3 inhibitor, produced a significant reduction of mEPSC amplitude (control, 21.1 ± 1.1 pA, $n = 13$; SB216763, 17.3 ± 0.7 pA, $n = 13$, $p < 0.01$, ANOVA, Fig. 1*C*). Dose-response experiments (Fig. 1*B*) indicated that 10–40 μM SB216763 inhibited mEPSC amplitude to a similar extent (~20%). Another GSK-3 inhibitor, Li_2CO_3 (1 mM, 10 min), also significantly suppressed mEPSC amplitude (control, 21.2 ± 0.8 pA, $n = 15$; SB216763, 17.9 ± 0.7 pA, $n = 15$, $p < 0.01$, ANOVA, Fig. 1*C*). Application of the selective AMPAR blocker 6-cyano-7-nitroquinoxaline-2,3-dione (10 μM) completely eliminated mEPSC (supplemental Fig. 1). These results suggest that inhibiting GSK-3 reduces AMPAR-mediated synaptic responses.

To further determine the role of GSK-3 in the regulation of synaptic AMPAR currents, we knocked down GSK-3 expression in cultured cortical neurons by transfecting an siRNA directed against GSK-3α or GSK-3β (15). GFP was co-transfected with GSK-3 siRNA. As shown in Fig. 1, *D* and *E*, significantly ($p < 0.01$, ANOVA) smaller mEPSC amplitude was found in neurons transfected with GSK-3β siRNA (17.8 ± 0.6 pA, $n = 9$) or GSK-3α plus GSK-3β siRNAs (17.4 ± 0.6 pA, $n = 12$) when compared with GFP-transfected neurons (22.1 ± 1.1 pA, $n = 14$) or GSK-3α siRNA-transfected neurons (22.7 ± 0.7 pA, $n = 5$). These results suggest that cellular knockdown of GSK-3β decreases AMPAR synaptic responses.

Given the effect of GSK-3 inhibitors on AMPARs, we would like to know the natural stimulus that could activate this pathway. Insulin has been found to induce GSK-3 inhibition via protein kinase B (PKB, also called AKT) signaling (22). Thus, we examined the effect of insulin on mEPSC. As shown in Fig. 1, *F* and *G*, application of insulin (0.5 μM, 10 min) caused a significant reduction of mEPSC amplitude (control, 21.3 ± 0.7 pA, $n = 23$; insulin, 17.6 ± 0.9 pA, $n = 12$, $p < 0.01$, ANOVA) and occluded the effect of SB216763 (insulin + SB216763, 16.6 ± 0.5 pA, $n = 11$). It suggests that

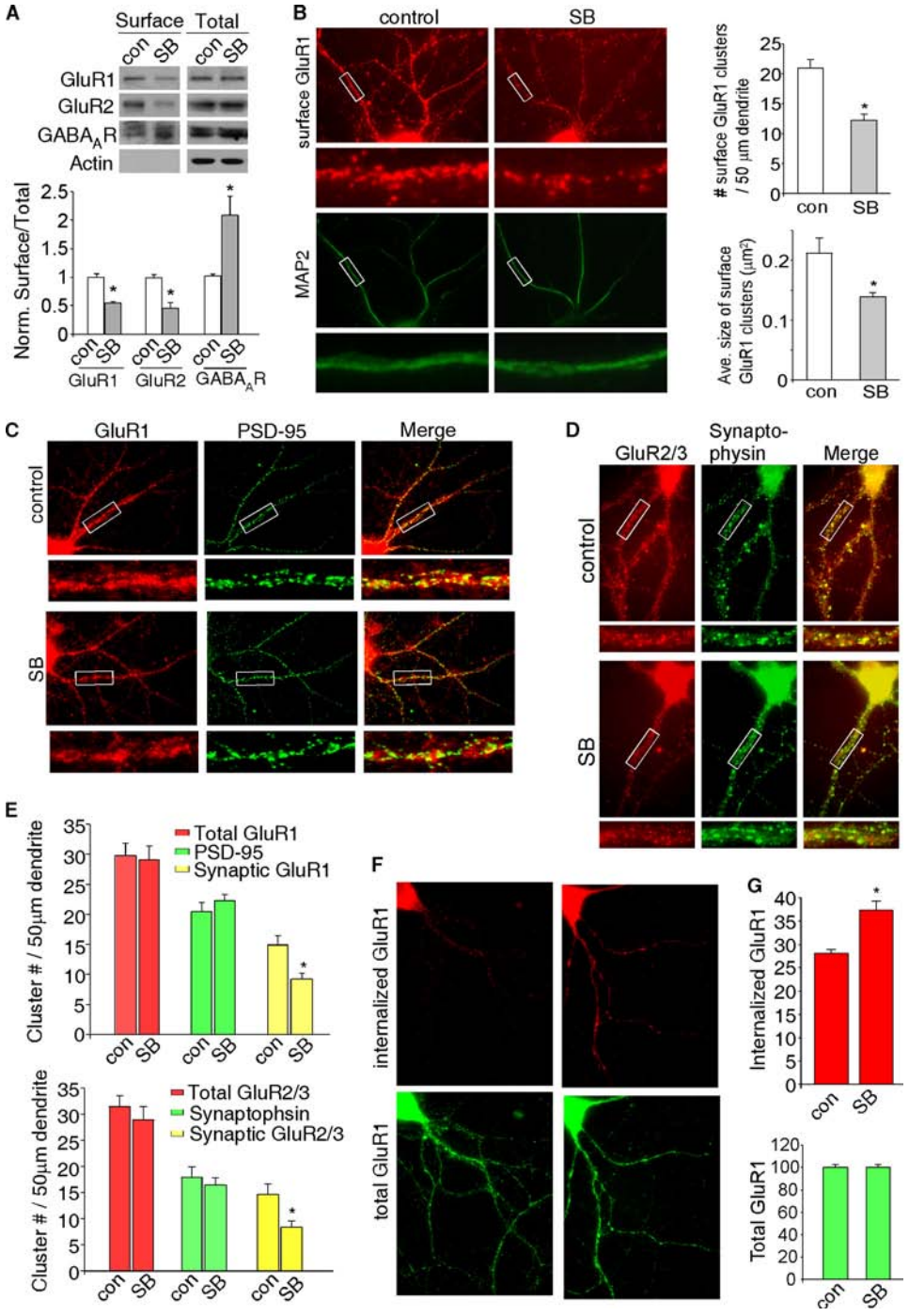

FIGURE 2. **Inhibiting GSK-3 reduces AMPAR surface expression and increases AMPAR internalization.** *A*, immunoblots showing the level of surface and total GluR1, GluR2, and $GABA_A$ receptor ($GABA_AR$) β2/3 subunits in cortical slices treated without or with SB216763 (*SB*, 10 μM, 10 min). *Bottom*, quantitation of the surface GluR1, GluR2, and $GABA_A$ receptor β2/3 expression. *con*, control. *, $p < 0.05$, Student's *t* test. *B*, immunocytochemical images of surface GluR1 staining in cultured cortical neurons (DIV 18) treated either with DMSO (*control*) or with SB21763 (10 μM, 10 min). Following surface GluR1 labeling, neurons were permeabilized and co-stained with MAP2. Enlarged versions of the *boxed regions* of dendrites are also shown. *Right*, quantitative analysis of surface GluR1 clusters (density, size) along dendrites in control or SB216763-treated neurons. *Ave. size*, average size. *, $p < 0.01$, Student's *t* test. *C–E*, immunocytochemical images (*C* and *D*) and quantitative analysis (*E*) of synaptic GluR1 clusters (PSD-95 co-localized, *yellow puncta*) or synaptic GluR2/3 clusters (synaptophysin co-localized, *yellow puncta*) in cortical cultures treated with DMSO (*control*) or SB216763 (10 μM, 10 min). Enlarged versions of the *boxed regions* of dendrites are also shown. *, $p < 0.01$, Student's *t* test. *F* and *G*, immunocytochemical images (*F*) and quantitative analysis (*G*) of internalized and total GluR1 in cortical cultures treated with DMSO (control) or SB216763 (10 μM, 10 min). *, $p < 0.01$, Student's *t* test.

activation of insulin signaling could suppress AMPAR synaptic responses via inhibiting GSK-3.

GSK-3 Regulates the Surface Expression and Internalization of AMPA Receptors—To test whether the GSK-3 regulation of mEPSC amplitude can be accounted for by the altered number of AMPA receptors on the cell membrane, we first performed surface biotinylation experiments to measure levels of surface GluR1. Surface proteins were labeled with sulfo-NHS-LC-biotin, and then biotinylated surface proteins were separated from non-labeled intracellular proteins by reaction with NeutrAvidin beads. Surface and total proteins were subjected to electrophoresis and probed with anti-GluR1 antibody. As shown in Fig. 2*A*, treatment of cortical neurons with SB216763 (10 μM, 10 min) significantly decreased the level of surface GluR1 (54.9 ± 2.3% of control, $n = 3$; $p < 0.01$, *t* test) and surface GluR2 (45.3 ± 10.0% of control, $n = 4$; $p < 0.01$, *t* test), whereas the level of total GluR1 and GluR2 was unchanged. In contrast, surface $GABA_A$ receptors were significantly increased by SB216763 treatment (2.09- ± 0.33-fold of control, $n = 4$; $p < 0.05$, *t* test), consistent with the recruitment of functional $GABA_A$ receptors to postsynaptic domains by insulin (23).

To further demonstrate the change in surface AMPARs by inhibiting GSK-3, we carried out a quantitative surface immunostaining assay in cortical cultures. The surface distribution of GluR1 was assessed by immunostaining with an antibody against the extracellular N-terminal domain of GluR1 in non-permeabilized conditions. As shown in Fig. 2*B*, application of SB216763 (10 μM, 10 min) caused a significant reduction of surface GluR1 cluster density (number of clusters/50 μm of dendrite, control, 21.0 ± 1.4, $n = 26$; SB216763, 12.3 ± 1.0, $n = 27$; $p < 0.01$, *t* test) and cluster size (control, 0.21 ± 0.03 μm^2, $n = 26$; SB216763, 0.14 ± 0.01 μm^2, $n = 27$; $p < 0.01$, *t*

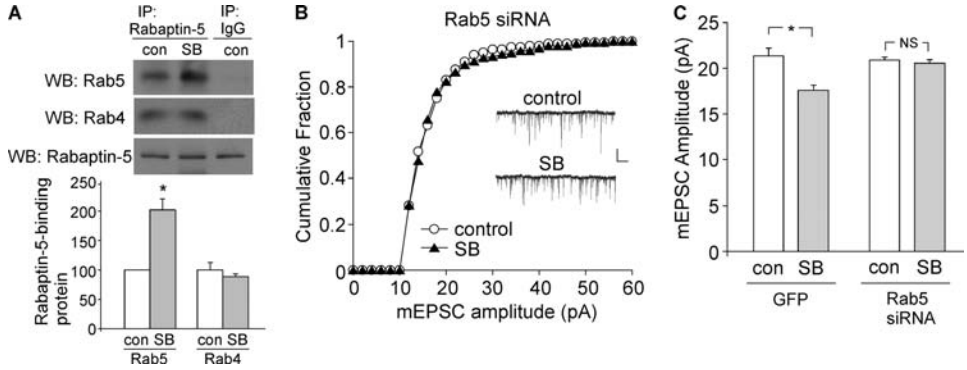

FIGURE 3. **GSK-3 regulation of synaptic AMPA activity requires Rab5 activation.** *A*, *top panel*, co-immunoprecipitation (*IP*) blots showing the level of active (Rabaptin-5-bound) Rab5 or Rab4 in cortical slices without or with SB216763 (*SB*) treatment (10 μM, 10 min). *con*, control; *WB*, Western blot. *Lower panel*, quantification showing the level of Rabaptin-5-bound (active) Rab5 or Rab4. *, $p < 0.01$, Student's *t* test. *B*, cumulative plots of mEPSC amplitude distribution before (*control*) and after SB216763 treatment (10 μM, 10 min) in a cultured cortical neuron transfected with Rab5 siRNA. *Inset*, representative mEPSC traces. *Scale bar*, 20 pA, 1 s. *C*, bar graphs showing the effect of SB216763 on mEPSC amplitude in neurons transfected with GFP or Rab5 siRNA. *, $p < 0.01$, ANOVA.

test). These data suggest that inhibiting GSK-3 reduces AMPAR surface expression.

To provide more direct evidence on GSK-3 regulation of AMPARs at synapses, we measured the synaptic AMPAR clusters, as indicated by GluR1 co-localized with the synaptic marker PSD-95. As shown in Fig. 2, *C* and *E*, a significant decrease of synaptic GluR1 (co-localized with PSD-95) cluster density (number of clusters/50 μm of dendrite) was observed in SB216763 (10 μM, 10 min)-treated cultures (control, 14.9 ± 1.5, $n = 26$; SB216763, 9.2 ± 0.9, $n = 25$, $p < 0.01$, *t* test), whereas the total GluR1 or PSD95 clusters were not altered by SB216763 treatment. Similarly, synaptic GluR2/3 (co-localized with synaptophysin) cluster density was also significantly decreased in SB216763-treated cultures (control, 14.7 ± 2.0, $n = 27$; SB216763, 8.4 ± 1.1, $n = 36$, $p < 0.01$, *t* test), whereas the total GluR2/3 or synaptophysin clusters were not altered (Fig. 2, *D* and *E*). It suggests that inhibiting GSK-3 reduces the number of AMPARs at synapses, which may account for the reduction of mEPSC amplitude by GSK-3 inhibitors.

We also performed immunocytochemical experiments to detect AMPAR internalization in cultured cortical neurons. Surface AMPARs were first stained with an antibody to the extracellular region of GluR1 subunit, and then following the treatment with GSK-3 inhibitors, surface-bound antibodies were stripped away so that only internalized AMPARs were visualized. As shown in Fig. 2, *F* and *G*, SB216763 (10 μM, 10 min) treatment caused a significant increase in the fluorescence intensity of internalized GluR1 on neuronal dendrites (control, 28.1 ± 0.7, $n = 28$; SB216763, 37.3 ± 2.1, $n = 30$; $p < 0.01$, *t* test). It suggests that inhibiting GSK-3 increases the internalization of AMPARs, which may result in the reduction of AMPARs at synaptic membrane.

GSK-3 Regulation of AMPARs Involves the Stimulation of the GDI-Rab5 Complex—To understand the potential mechanism underlying GSK-3 regulation of AMPAR internalization, we examined the role of Rab5, a key mediator of protein transport from plasma membrane to early endosomes during clathrin-dependent endocytosis (24). First, we examined whether GSK-3 could regulate the activity of this small GTPase. Because Rabaptin-5, a molecule identified as a Rab5-interacting protein, binds to only the GTP-bound, active form of Rab5 at its C terminus (25), we measured Rabaptin-5-bound Rab5 by co-immunoprecipitation experiments to indicate its activity level. As shown in Fig. 3*A*, SB216763 (10 μM, 10 min) treatment of cortical slices induced a significant increase of Rab5 activity, as indicated by the elevated level of Rabaptin-5-bound Rab5 (2.02- ± 0.19-fold of control, $n = 3$, $p < 0.01$, *t* test). To test the specificity of Rab5 involvement, we also examined Rab4, which mediates receptor recycling between early endosomes and the plasma membrane. Rabaptin-5 binds to the active form of Rab4 at its N terminus (25). As shown in Fig. 3*A*, the Rabaptin-5-bound (active) Rab4 was not significantly changed by GSK-3 inhibition.

To test whether Rab5-dependent endocytosis of AMPA receptors is involved in GSK-3 regulation of mEPSC, we knocked down Rab5 expression in cultured cortical neurons by transfecting with an siRNA against Rab5 (GFP was co-transfected). As shown in Fig. 3, *B* and *C*, SB216763 (10 μM, 10 min) had little effect on mEPSC amplitude in neurons (GFP+) transfected with Rab5 siRNA (control, 20.9 ± 0.4 pA, $n = 11$; SB216763, 20.6 ± 0.4 pA, $n = 11$), whereas it produced a significant reduction of mEPSC amplitude in neurons transfected with GFP alone (control, 21.4 ± 0.8 pA, $n = 11$; SB216763, 17.6 ± 0.6 pA, $n = 11$, $p < 0.01$, ANOVA). It suggests that GSK-3 regulates AMPAR trafficking and function via a Rab5-dependent mechanism.

Next, we sought to determine the mechanism underlying GSK-3 regulation of Rab5-mediated AMPAR internalization. It is known that the recycling of Rab proteins between a membrane-bound and a cytosolic state is dependent on the GDP dissociation inhibitor (26). Previous studies have found that the formation of GDI-Rab complex can be altered by phosphorylation of GDI (27, 28), leading to accelerated exocytosis or endocytosis. Thus, we tested the potential involvement of GDI in GSK-3 regulation of AMPARs.

First, we examined whether GSK-3 alters the formation of the GDI-Rab5 complex. As shown in the co-immunoprecipitation assay (Fig. 4*A*), SB216763 (10 μM, 10 min) treatment significantly increased the amount of Rab5 that binds to GDI (1.63- ± 0.13-fold of control, $n = 3$, $p < 0.01$, *t* test). It suggests that inhibiting GSK-3 increases the formation of GDI-Rab5 complex, which may account for the increased endocytic trafficking of surface AMPA receptors.

To further test the role of GDI in GSK-3 regulation of AMPARs, we dialyzed neurons with an antibody against GDI to block the function of endogenous GDI. As shown in Fig. 4*B*, the GDI antibody (4 μg/ml) produced a significant decrease of mEPSC amplitude in cultured cortical neurons (control, 21.0 ±

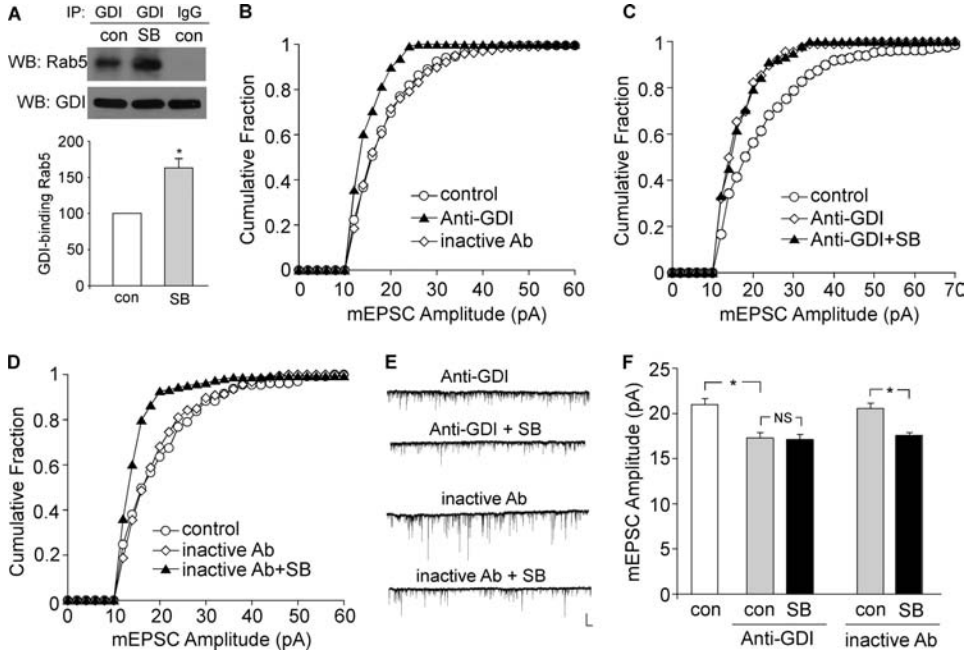

FIGURE 4. **The GDI-Rab5 complex is involved in GSK-3 regulation of synaptic AMPAR activity.** *A*, *top panel*, co-immunoprecipitation (*IP*) blots showing the level of Rab5 that binds to GDI in cortical slices treated without or with SB216763 (*SB*, 10 μM, 10 min). *con*, control; *WB*, Western blot. *Lower panel*, quantification showing the level of GDI-bound Rab5. *, $p < 0.01$, Student's *t* test. *B*, cumulative plots of mEPSC amplitude distribution showing the effect of GDI antibody (4 μg/ml) or a heat-inactivated antibody. *C* and *D*, cumulative plots of mEPSC amplitude distribution showing the effect of SB216763 (10 μM, 10 min) in cultured cortical neurons dialyzed with GDI antibody (*C*) or the inactive antibody (*D*, *Inactive Ab*). *E*, representative mEPSC traces. *Scale bar*, 20 pA, 1 s. *F*, bar graphs showing the mEPSC amplitude before and after SB216763 treatment in the absence or presence of different antibodies. *, $p < 0.01$, ANOVA; *NS*, not significant.

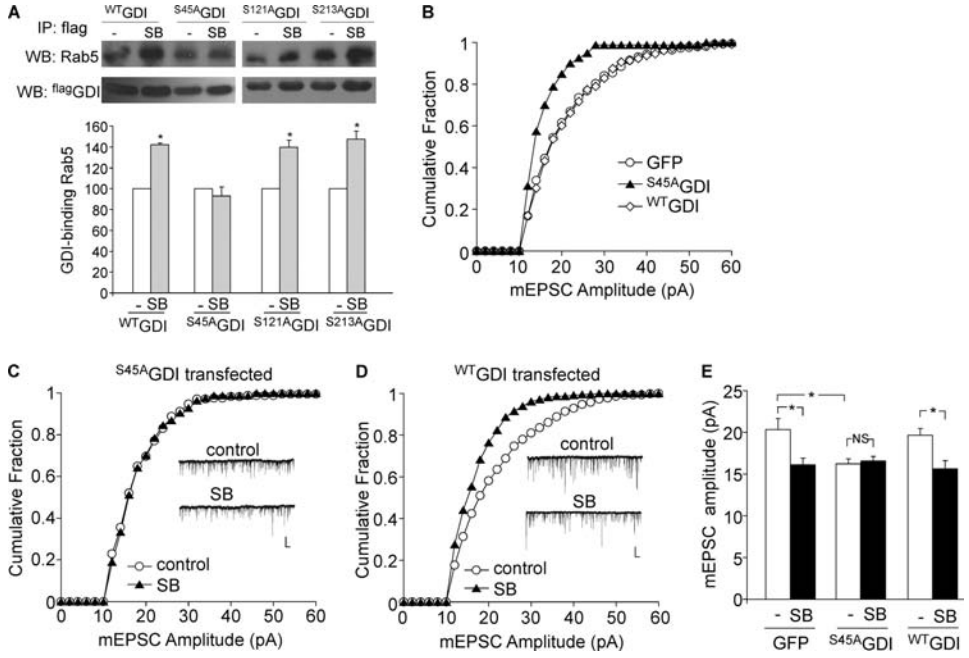

FIGURE 5. **Phosphorylation of GDI at Ser-45 is required for GSK-3 regulation of synaptic AMPA activity.** *A*, *top panel*, co-immunoprecipitation (*IP*) blots showing the level of Rab5 that binds to GDI in HEK293 cells transfected with FLAG-tagged wild-type GDI or its three mutants, S45A, S121A, and S213A. After transfection, cells were treated without or with SB216763 (*SB*, 10 μM) for 10 min. *WB*, Western blot. *Lower panel*, quantification showing the level of GDI-bound Rab5 in control *versus* SB216763-treated HEK293 cells transfected with different GDI constructs. *, $p < 0.01$, ANOVA. *B*, cumulative plots of mEPSC amplitude distribution in cultured cortical neurons transfected with GFP alone, ^{S45A}GDI, or ^{WT}GDI. *C* and *D*, cumulative plots of mEPSC amplitude distribution showing the effect of SB216763 (10 μM, 10 min) in neurons transfected with ^{S45A}GDI (*C*) or ^{WT}GDI (*D*). *Inset*, representative mEPSC traces. *Scale bar*, 20 pA, 1 s. *E*, bar graphs showing the mEPSC amplitude in control and SB216763-treated neurons transfected with different constructs. *, $p < 0.01$, ANOVA; *NS*, not significant.

0.6 pA, $n = 12$; anti-GDI antibody, 17.3 ± 0.6 pA, $n = 12$, $p < 0.01$, ANOVA, Fig. 4*F*). Moreover, in neurons dialyzed with anti-GDI antibody, subsequent application of SB216763 (10 μM, 10 min) failed to further decrease mEPSC amplitude (Fig. 4, *C* and *E*, 17.1 ± 0.6 pA, $n = 12$, Fig. 4*F*). In contrast, the heat-inactivated antibody did not alter mEPSC amplitude (Fig. 4*B*) and failed to occlude the reducing effect of SB216763 (Fig. 4, *D* and *E*, control, 20.6 ± 0.6 pA, $n = 5$; SB216763, 17.6 ± 0.3 pA, $n = 5$, $p < 0.01$, ANOVA, Fig. 4*F*). These results suggest that GDI is required for GSK-3 regulation of AMPA receptors.

GDI Phosphorylation at Ser-45 Is Required for GSK-3 Regulation of AMPAR Synaptic Activity and Surface Expression—GDI contains 26 Ser residues, and Ser-45, Ser-121, and Ser-213 have been predicted to face the outer surface of the molecule based on its three-dimensional structure (28, 29). To identify the phosphorylation site that is critically involved in GSK-3 regulation of AMPARs, we transfected HEK293 cells with FLAG-tagged wild-type GDI or non-phosphorylatable GDI mutants, S45A, S121A, and S213A. After transfection, cells were treated with SB216763. Cell lysates were subjected to a co-immunoprecipitation assay to detect the GDI-Rab5 complex. As shown in Fig. 5*A*, SB216763 (10 μM, 10 min) treatment significantly increased the amount of Rab5 that binds to WT-GDI, S121A-GDI, or S213A-GDI but not to S45A-GDI. It suggests that GSK-3 regulation of the GDI-Rab5 complex requires an intact Ser-45 phosphorylation site on GDI.

We further investigated whether GDI phosphorylation at Ser-45 could influence synaptic AMPAR activity and its regulation by GSK-3 in cortical cultures. As shown in Fig. 5*B*, when compared with neurons transfected with GFP alone, transfecting ^{S45A}GDI, but not ^{WT}GDI, caused a significant decrease of mEPSC amplitude. Furthermore,

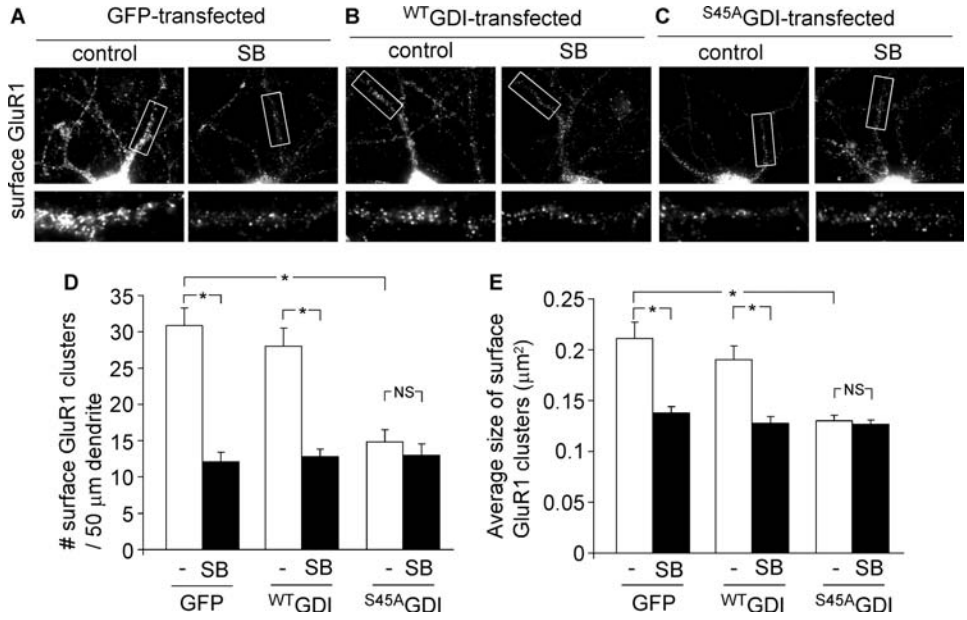

FIGURE 6. **Phosphorylation of GDI at Ser-45 is required for GSK-3 regulation of AMPAR surface expression.** *A–C*, immunocytochemical images of surface GluR1 staining in control or SB216763 (*SB*, 10 μM, 10 min)-treated neurons transfected with GFP alone (*A*), ^{WT}GDI (*B*), or ^{S45A}GDI (*C*). *D* and *E*, cumulative data showing the surface GluR1 cluster density and size in control *versus* SB216763-treated neurons transfected with different constructs. *, $p < 0.01$, ANOVA.

the reducing effect of SB216763 on mEPSC amplitude was lost in neurons transfected with ^{S45A}GDI (Fig. 5*C*, ^{S45A}GDI, 16.2 ± 0.6 pA, $n = 14$; ^{S45A}GDI + SB216763, 16.5 ± 0.6, $n = 14$, Fig. 5*E*) but not in those transfected with ^{WT}GDI (Fig. 5*D*, ^{WT}GDI, 19.7 ± 0.8 pA, $n = 14$; ^{WT}GDI + SB216763, 15.6 ± 1.0 pA, $n = 14$, $p < 0.01$, ANOVA, Fig. 5*E*) or GFP alone (GFP, 20.3 ± 1.3 pA, $n = 13$; GFP ± SB216763, 16.1 ± 0.8 pA, $n = 13$, $p < 0.01$, ANOVA, Fig. 5*E*). These data suggest that GSK-3 regulation of synaptic AMPAR currents requires an intact Ser-45 phosphorylation site on GDI.

To confirm the role of GDI phosphorylation in GSK-3 regulation of AMPAR trafficking, we performed immunocytochemical experiments to measure AMPAR surface expression in neurons transfected with wild-type or mutant GDI. As shown in Fig. 6, *A* and *B*, in GFP- or ^{WT}GDI-transfected neurons, SB216763 treatment (10 μM, 10 min) significantly decreased surface GluR1 cluster density (number of clusters/50 μm of dendrite, GFP, 30.9 ± 2.4, $n = 31$; GFP + SB216763, 12.1 ± 1.3, $n = 24$; ^{WT}GDI, 28.0 ± 2.5, $n = 23$; ^{WT}GDI + SB216763, 12.8 ± 1.0, $n = 21$, $p < 0.01$, ANOVA, Fig. 6*D*) and cluster size (GFP, 0.21 ± 0.02 μm^2, $n = 31$; GFP + SB216763, 0.14 ± 0.01 μm^2, $n = 24$; ^{WT}GDI, 0.19 ± 0.01 μm^2, $n = 23$; ^{WT}GDI + SB216763, 0.13 ± 0.01 μm^2, $n = 21$, $p < 0.01$, ANOVA, Fig. 6*E*). Transfecting ^{S45A}GDI (Fig. 6*C*) caused a significant decrease of surface GluR1 clusters and occluded the reducing effect of SB216763 (cluster density, ^{S45A}GDI, 14.8 ± 1.7, $n = 31$; ^{S45A}GDI + SB216763, 13.0 ± 1.5, $n = 24$; cluster size, ^{S45A}GDI, 0.13 ± 0.01 μm^2, $n = 31$; ^{S45A}GDI + SB216763, 0.13 ± 0.01 μm^2, $n = 24$, Fig. 6*E*). These data suggest that GDI phosphorylation at Ser-45 is important for the membrane trafficking of AMPARs and that GSK-3 regulates AMPAR surface expression via a mechanism dependent on GDI phosphorylation at Ser-45.

DISCUSSION

In this study, we have examined the synaptic function of GSK-3, a multifunctional kinase implicated in various neurological disorders (9, 10, 14). We found that GSK-3 inhibitors caused a significant reduction of AMPAR synaptic responses, which was accompanied by the loss of AMPAR surface expression and the increase of AMPAR internalization. It is known that the redistribution of postsynaptic AMPARs plays a key role in controlling excitatory synaptic efficacy (17, 18). An earlier study has found that insulin accelerates the clathrin-dependent endocytosis of AMPA receptors, resulting in long term depression of AMPAR-mediated synaptic transmission in hippocampal CA1 neurons (30). Because insulin can induce GSK-3 inhibition via PKB/Akt signaling (22) and insulin mimics and occludes the effect of GSK-3 inhibitors on mEPSC amplitude, it suggests that insulin may facilitate the internalization of AMPARs via GSK-3 inhibition.

Mounting evidence suggests that the trafficking of AMPARs is controlled by the Rab family of small GTPases, a key coordinator of intracellular transport steps in exocytic and endocytic pathways (31, 32). Rab5, which mediates the transport from plasma membrane to early endosomes (24), is involved in clathrin-dependent AMPAR internalization (33, 34). Rab11, which mediates recycling from recycling endosomes to plasma membrane (35), controls the supply of AMPARs during long term potentiation (36, 37). Rab8, which is associated with trans-Golgi network membranes, plays a role in AMPAR transport to the spine surface (38). In this study, we have found that inhibiting GSK-3 increases Rab5 activity and that Rab5 knockdown prevents GSK-3 from regulating mEPSC amplitude. This suggests that GSK-3 inhibitors may reduce AMPAR synaptic responses by enhancing Rab5-mediated AMPAR internalization.

How does inhibiting GSK-3 signaling lead to the activation of Rab5? One possibility is through GDI, an important class of proteins regulating the functional cycle of Rab between a membrane-bound and a cytosolic state (31). GDI extracts the inactive GDP-bound Rab from membranes and acts as a cytosolic chaperone of Rab (39, 40). Interestingly, the formation of GDI-Rab complex can be altered by phosphorylation of GDI (27, 28, 41), leading to accelerated exocytosis or endocytosis. For example, p38 MAPK activates GDI and stimulates the formation of GDI-Rab5 complex by phosphorylating GDI on Ser-121, therefore facilitating the delivery of Rab5 from endosomes to the plasma membrane and accelerating endocytosis (28). In this study, we have found that inhibiting GSK-3 increases the GDI-Rab5 complex, an effect requiring the intact Ser-45 phosphor-

ylation site on GDI. The non-phosphorylatable ^{S45A}GDI decreases AMPAR trafficking/function and occludes the reducing effect of GSK-3 inhibitors. It suggests that GSK-3 regulation of AMPARs is through a mechanism involving GDI phosphorylation at Ser-45 and GDI-Rab5 complex formation.

In summary, we have revealed a potential mechanism for GSK-3 regulation of AMPARs. Our results suggest that constitutively active endogenous GSK-3 plays an important role in maintaining AMPARs at the synaptic membrane. It is conceivable that dysregulation of glutamatergic transmission by impaired GSK-3 signaling may be a key pathophysiological mechanism for those mental illnesses involving GSK-3.

Acknowledgments—We thank Xiaoqing Chen and Dr. Eunice Yuen for excellent technical support.

REFERENCES

1. Welsh, G. I., Wilson, C., and Proud, C. G. (1996) *Trends Cell Biol.* **6,** 274–279
2. Frame, S., and Cohen, P. (2001) *Biochem. J.* **359,** 1–16
3. Jope, R. S., and Johnson, G. V. (2004) *Trends Biochem. Sci.* **29,** 95–102
4. Zhou, F. Q., and Snider, W. D. (2005) *Science* **308,** 211–214
5. Jiang, H., Guo, W., Liang, X., and Rao, Y. (2005) *Cell* **120,** 123–135
6. Kim, W. Y., Wang, X., Wu, Y., Doble, B. W., Patel, S., Woodgett, J. R., and Snider, W. D. (2009) *Nat. Neurosci.* **12,** 1390–1397
7. Woodgett, J. R. (1990) *EMBO J.* **9,** 2431–2438
8. Cross, D. A., Alessi, D. R., Cohen, P., Andjelkovich, M., and Hemmings, B. A. (1995) *Nature* **378,** 785–789
9. Coyle, J. T., and Duman, R. S. (2003) *Neuron* **38,** 157–160
10. Phiel, C. J., and Klein, P. S. (2001) *Annu. Rev. Pharmacol. Toxicol.* **41,** 789–813
11. Emamian, E. S., Hall, D., Birnbaum, M. J., Karayiorgou, M., and Gogos, J. A. (2004) *Nat. Genet.* **36,** 131–137
12. Phiel, C. J., Wilson, C. A., Lee, V. M., and Klein, P. S. (2003) *Nature* **423,** 435–439
13. Hong, M., Chen, D. C., Klein, P. S., and Lee, V. M. (1997) *J. Biol. Chem.* **272,** 25326–25332
14. Meijer, L., Flajolet, M., and Greengard, P. (2004) *Trends Pharmacol. Sci.* **25,** 471–480
15. Chen, P., Gu, Z., Liu, W., and Yan, Z. (2007) *Mol. Pharmacol.* **72,** 40–51
16. Peineau, S., Taghibiglou, C., Bradley, C., Wong, T. P., Liu, L., Lu, J., Lo, E., Wu, D., Saule, E., Bouschet, T., Matthews, P., Isaac, J. T., Bortolotto, Z. A., Wang, Y. T., and Collingridge, G. L. (2007) *Neuron* **53,** 703–717
17. Malinow, R., and Malenka, R. C. (2002) *Annu. Rev. Neurosci.* **25,** 103–126
18. Collingridge, G. L., Isaac, J. T., and Wang, Y. T. (2004) *Nat. Rev. Neurosci.* **5,** 952–962
19. Yuen, E. Y., Jiang, Q., Chen, P., Gu, Z., Feng, J., and Yan, Z. (2005) *J. Neurosci.* **25,** 5488–5501
20. Gu, Z., Liu, W., and Yan, Z. (2009) *J. Biol. Chem.* **284,** 10639–10649
21. Gu, Z., Jiang, Q., Fu, A. K., Ip, N. Y., and Yan, Z. (2005) *J. Neurosci.* **25,** 4974–4984
22. Cohen, P., and Frame, S. (2001) *Nat. Rev. Mol. Cell Biol.* **2,** 769–776
23. Wan, Q., Xiong, Z. G., Man, H. Y., Ackerley, C. A., Braunton, J., Lu, W. Y., Becker, L. E., MacDonald, J. F., and Wang, Y. T. *Nature* (1997) **388,** 686–690
24. Bucci, C., Parton, R. G., Mather, I. H., Stunnenberg, H., Simons, K., Hoflack, B., and Zerial, M. (1992) *Cell* **70,** 715–728
25. Vitale, G., Rybin, V., Christoforidis, S., Thornqvist, P., McCaffrey, M., Stenmark, H., and Zerial, M. (1998) *EMBO J.* **17,** 1941–1951
26. Sasaki, T., Kikuchi, A., Araki, S., Hata, Y., Isomura, M., Kuroda, S., and Takai, Y. (1990) *J. Biol. Chem.* **265,** 2333–2337
27. Shisheva, A., Chinni, S. R., and DeMarco, C. (1999) *Biochemistry* **38,** 11711–11721
28. Cavalli, V., Vilbois, F., Corti, M., Marcote, M. J., Tamura, K., Karin, M., Arkinstall, S., and Gruenberg, J. (2001) *Mol. Cell* **7,** 421–432
29. Schalk, I., Zeng, K., Wu, S. K., Stura, E. A., Matteson, J., Huang, M., Tandon, A., Wilson, I. A., and Balch, W. E. (1996) *Nature* **381,** 42–48
30. Man, H. Y., Lin, J. W., Ju, W. H., Ahmadian, G., Liu, L., Becker, L. E., Sheng, M., and Wang, Y. T. (2000) *Neuron* **25,** 649–662
31. Zerial, M., and McBride, H. (2001) *Nat. Rev. Mol. Cell Biol.* **2,** 107–117
32. Pfeffer, S. R. (2001) *Trends Cell Biol.* **11,** 487–491
33. Brown, T. C., Tran, I. C., Backos, D. S., and Esteban, J. A. (2005) *Neuron* **45,** 81–94
34. Zhong, P., Liu, W., Gu, Z., and Yan, Z. (2008) *J. Physiol.* **586,** 4465–4479
35. Ullrich, O., Reinsch, S., Urbé, S., Zerial, M., and Parton, R. G. (1996) *J. Cell Biol.* **135,** 913–924
36. Park, M., Penick, E. C., Edwards, J. G., Kauer, J. A., and Ehlers, M. D. (2004) *Science* **305,** 1972–1975
37. Brown, T. C., Correia, S. S., Petrok, C. N., and Esteban, J. A. (2007) *J. Neurosci.* **27,** 13311–13315
38. Gerges, N. Z., Backos, D. S., and Esteban, J. A. (2004) *J. Biol. Chem.* **279,** 43870–43878
39. Shisheva, A., Südhof, T. C., and Czech, M. P. (1994) *Mol. Cell Biol.* **14,** 3459–3468
40. Novick, P., and Zerial, M. (1997) *Curr. Opin. Cell Biol.* **9,** 496–504
41. Steele-Mortimer, O., Gruenberg, J., and Clague, M. J. (1993) *FEBS Lett.* **329,** 313–318